EVALUATING SPECTRAL MEASURES DERIVED FROM AIRBORNE MULTISPECTRAL IMAGERY FOR DETECTING COTTON ROOT ROT

C. Yang

Southern Plains Agricultural Research Center
USDA-ARS
College Station, Texas

G.N. Odvody, C.J. Fernandez, J.A. Landivar

Texas AgriLife Research and Extension Center
Corpus Christi, Texas

R.L. Nichols

Cotton Incorporated
Cary, North Carolina

ABSTRACT

Cotton root rot, caused by the soilborne fungus *Phymatotrichopsis omnivore*, is one of the most destructive plant diseases occurring throughout the southwestern United States. This disease has plagued the cotton industry for more than 100 years, but effective practices for its control are still lacking. Recent research has shown that a commercial fungicide, flutriafol, has potential for the control of cotton root rot. To effectively and economically control this disease, it is necessary to identify infected areas within the field so that variable rate technology can be used to apply fungicide only to the infected areas. The objectives of this study were to evaluate two vegetation indices, the simple ratio index (SRI) and the normalized difference vegetation index (NDVI), and four supervised classification techniques, including minimum distance, Mahalanobis distance, maximum likelihood, and spectral angle mapper (SAM), for detecting cotton root rot from airborne multispectral imagery. One cotton field with a history of root rot infection in south Texas was selected for this study. Airborne multispectral imagery with blue, green, red and near-infrared bands was taken from the field shortly before harvest when infected areas were fully expressed for the 2011 growing season. The two VIs were derived from the multispectral imagery and then statistically grouped into infected and noninfected classes. The four-band image was classified into infected and non-infected zones using the four classifiers based on training samples from the image. Accuracy assessment on the two-zone classification maps showed that all six methods accurately identified root rot-infected areas within the field with accuracies from 94.5 to 96.5%. The results of this study will be useful for effective detection of cotton root rot and for site-specific management of this disease.

Keywords: Cotton root rot, airborne multispectral imagery, vegetation index, unsupervised classification.

INTRODUCTION

Cotton is an economically important crop that is highly susceptible to cotton root rot, a destructive plant disease that occurs throughout the southwestern U.S. Infected plants wilt and quickly die with the leaves attached to the plants (Smith et al., 1962). The symptoms usually begin during the period of rapid vegetative growth, are more visible during flowering and fruit development, and continue to increase through the growing season. Plants infected earlier in the growing season will die before bearing fruit, whereas infection occurring at later plant growth stages will reduce cotton yield and lower lint quality (Ezekiel and Taubenhaus, 1934; Yang et al., 2005).

Cotton root rot is an age-old problem and has plagued the cotton industry for more than 100 years. Despite decades of research efforts, effective practices to control this disease are still lacking. More recently, new fungicides have been evaluated and a commercial formulation of flutriafol (Topguard® - Cheminova, Inc., Wayne, NJ) was found to effectively control cotton root rot (Isakeit et al., 2009, 2010). To effectively and economically control this disease, it is necessary to identify infected areas within the field so that variable rate technology can be used to apply fungicide only to infected areas.

Remote sensing has been successfully used to map cotton root rot infections in cotton fields (Nixon et al., 1987; Yang et al. 2005, 2010). Preliminary work has been done to monitor the progression of the disease within a growing season or across different growing seasons (Yang et al., 2011). In previous studies, unsupervised classification directly applied to imagery has been used to identify root rot-infected areas. However, many other spectral measures and classification techniques may offer advantages. Therefore, the objectives of this study were to evaluate two most commonly used vegetation indices, the simple ration index (SRI) and the normalized difference vegetation index (NDVI), and four supervised classification techniques, including minimum distance, Mahalanobis distance, maximum likelihood, and spectral angle mapper (SAM), for detecting cotton root rot from airborne multispectral imagery.

METHODS

Study site

A center-pivot irrigated cotton field near Edroy, TX, (28°00′5″ N, 97°38′33″ W) was selected for this study. This field had a history of cotton root rot. Cotton and grain sorghum have been cropped alternately in the field and cotton was planted in the field in 2011.

Airborne multispectral image acquisition

An airborne four-camera imaging system described by Yang (2010) was used to acquire multispectral imagery. The system consists of four high resolution CCD digital cameras and a ruggedized PC equipped with a frame grabber and image acquisition software. The cameras are sensitive in the 400 to 1000 nm spectral range and provide 2048 × 2048 active pixels with 12-bit data depth. The four cameras are equipped with blue (430-470 nm), green (530-570 nm), red (630-670 nm), and near-infrared (NIR, 810-850 nm) bandpass interference filters, respectively. A Cessna 206 single-engine aircraft was used to acquire imagery from the field at an altitude of 3050 m (10000 ft) between 1130h and 1430h local time under sunny conditions on July 13, 2011. The ground pixel size achieved was approximately 0.9 m.

Image alignment and rectification

An image-to-image registration procedure based on the first-order polynomial transformation model was used to align the four individual band images in the composite image. The registered images were then georeferenced or rectified to the Universal Transverse Mercator (UTM), World Geodetic Survey 1984 (WGS-84), Zone 14, coordinate system based on a set of ground control points around the field located with a Trimble GPS Pathfinder ProXRS receiver (Trimble Navigation Limited, Sunnyvale, California). The root mean square (RMS) errors for rectifying the images using first-order transformation were approximately 2 m. All images were resampled to 1 m resolution using the nearest neighborhood technique. All procedures for image registration and rectification were performed using ERDAS Imagine (ERDAS Inc., Norcross, Georgia).

Vegetation Indices

The simple ratio index (SRI = NIR / Red) (Jordan, 1969) and the normalized difference vegetation index [NDVI = (NIR – Red) / (NIR + Red)] (Rouse et al., 1973), were calculated from the multispectral image. The SRI and NDVI images were then classified into two spectral classes using ISODATA (Iterative Self-Organizing Data Analysis) unsupervised classification (ERDAS, 2010). This method ensures that each pixel is assigned to the class that has the minimum spectral distance to the pixel. Thus the two vegetation index images were each classified into root rot-infected and noninfected zones. ERADAS Imagine was used for this analysis.

Supervised classification

Based on ground observations, cotton root rot was the only dominant stressor affecting the field, even though some minor biotic and abiotic stressors may have been present. However, since the fungus can cause such a devastating effect on the plants, it has a very unique signature on the airborne image compared with other stressors such as nutrient deficiencies and minor insect

damage. Therefore, the field can be classified into root rot-infected areas and noninfected areas.

Four supervised classification methods, including minimum distance, Mahalanobis distance, maximum likelihood, and spectral angle mapper (SAM), were applied to the four-band multispectral image. The minimum distance classifier uses the class means derived from the training data and assigns each pixel to the class that has the closest Euclidean distance from the pixel (Campbell, 2002). The Mahalanobis distance method is similar to minimum distance, except that the covariance matrix is used in the calculation (ERDAS, 2010). Each pixel is assigned to the class for which Mahalanobis distance is the smallest. Maximum likelihood classification assumes that the data for each class in each band are normally distributed and it calculates the probability that a given pixel belongs to a specific class (Richards, 1999). Each pixel is assigned to the class that has the highest probability (i.e., the maximum likelihood). Spectral angle mapper or SAM is a spectral classification technique that uses the n-dimensional angle to match pixels to endmembers (Kruse et al., 1993). The algorithm determines the spectral similarity between a pixel spectrum and an endmember spectrum by calculating the angle between them, treating them as vectors in a space with dimensionality equal to the number of bands. Each pixel is assigned to the endmember whose spectrum has the smallest spectral angle with the pixel spectrum.

For supervised training, a number of infected and noninfected areas were identified and digitized on the multispectral image as the training samples to represent respective classes. The numbers of digitized training pixels were 1927 for the infected class and 2265 for the noninfected class. The same circular ROI boundary was used to exclude the areas outside the boundary for image classification. Each classifier resulted in a two-class classification map. ENVI (Research Systems, Inc., Boulder, Colorado) was used for supervised classification.

Accuracy assessment

For accuracy assessment of the two vegetation index-based classification maps and the four supervised classification maps, 200 points were generated and assigned to the two classes in a stratified random pattern. Since the classes for a large majority of these points could be accurately determined from the color and color-infrared (CIR) images for the field, only a few points were located in the transitional areas where their classes could belong to either class. Error matrices for each classification map were generated by comparing the classified classes with the actual classes at these 200 points. Classification accuracy measures, including overall accuracy, kappa coefficient, producer's accuracy, user's accuracy, were calculated based on the error matrices (Congalton and Green, 1999).

RESULTS AND DISCUSSION

Figure 1 shows the normal color and CIR composite images acquired from the field shortly before harvest in 2011. On the normal color image, noninfected plants had a green color, whereas infected plant had a brownish or grayish tone.

On the CIR image, noninfected plants showed a reddish-magenta tone, while infected plants had a cyanish or light greenish color. Root rot-infected areas could be easily separated from the noninfected areas on both images, especially on the CIR image. Cotton root rot progressed across much of the field and continued to develop in the north edge of the field toward the later part of the growing season.

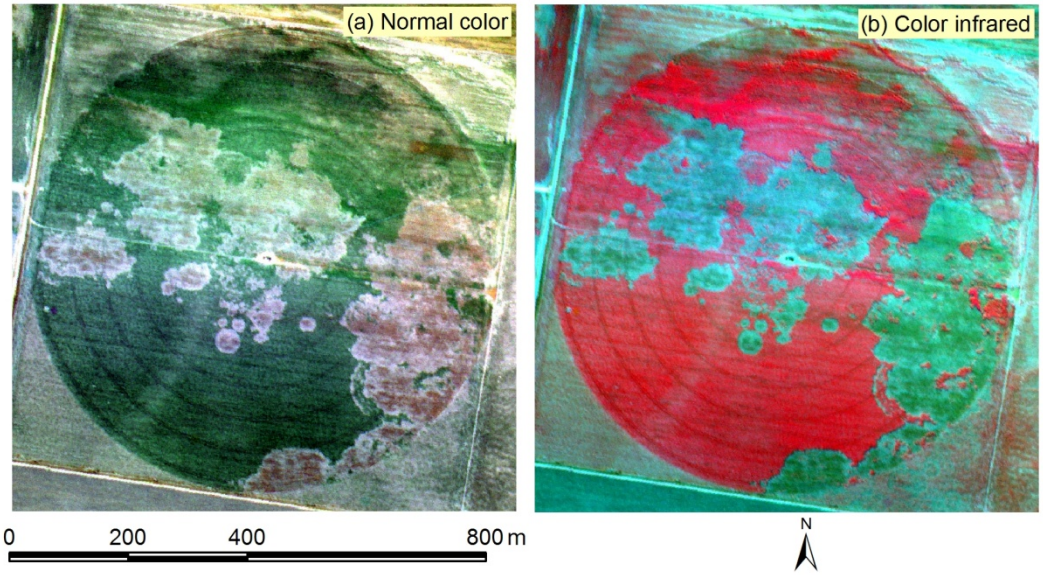

Fig. 1. Airborne normal color and color-infrared (CIR) images acquired from a 48.5-ha cotton root rot-infected cotton field near Edroy, TX in 2011.

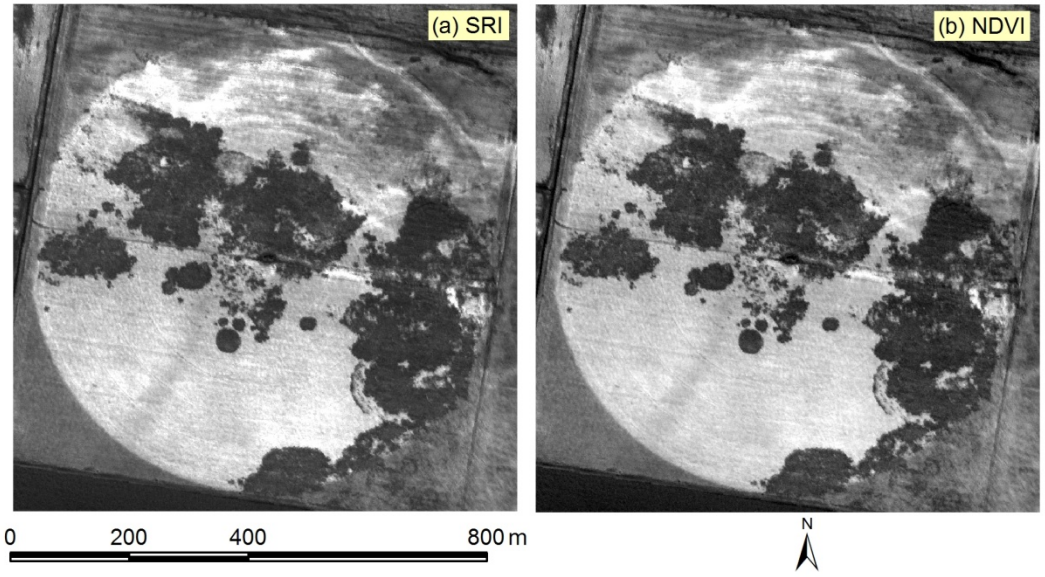

Fig. 2. Simple ratio index (SRI) image and normalized difference vegetation index (NDVI) image derived from a multispectral image for a 48.5-ha cotton root rot-infected cotton field near Edroy, TX in 2011.

Figure 2 shows the SRI and NDVI images derived from the multispectral image for the field. Infected areas had lower values and exhibited a dark grayish color. Noninfected areas had higher values and showed a light gray tone. The very dark color on the images represent areas with dead dry plants, whereas the slightly dark color in the north and northeast portion of the circular field indicate infected plants that were not completely dry. Both SRI and NDVI images reveal similar patterns.

Figure 3 shows the two-zone classification maps based on the two vegetation indices and the four supervised classifiers. A visual comparison of the classification maps and their respective color and CIR images indicated that all the classification maps effectively identify apparent root rot areas within the field and that there were minimal differences among them.

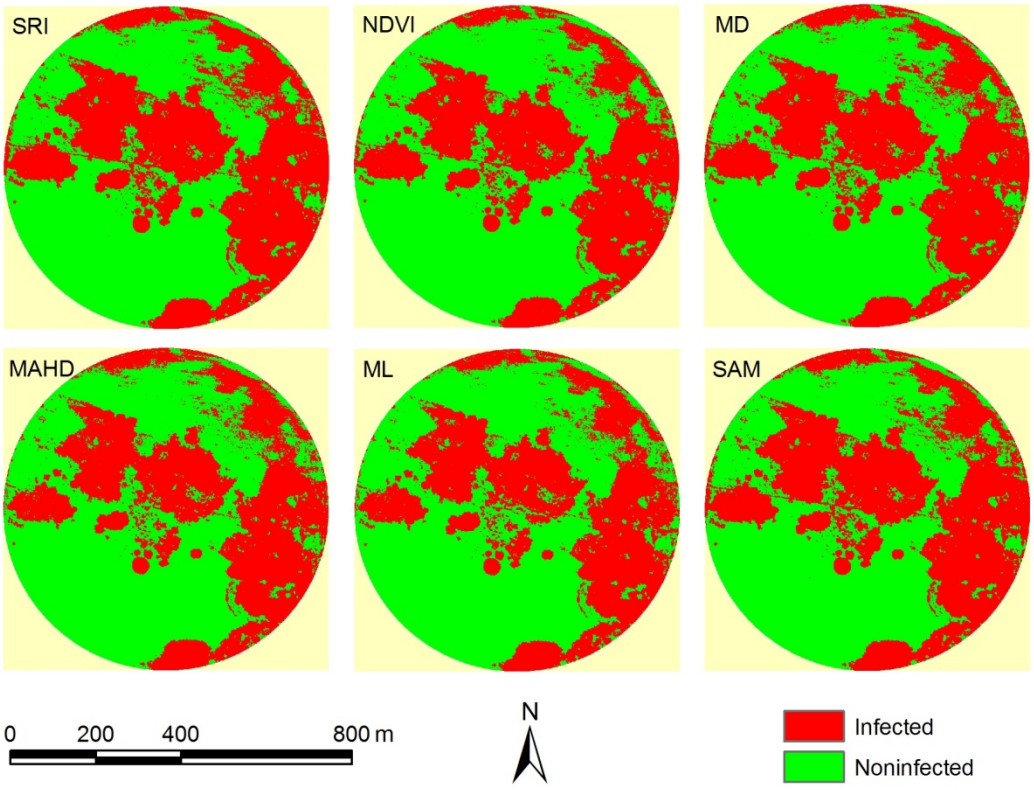

Fig. 3. Two-zone classification maps based on six methods from a four-band multispectral image of a 48.5-ha cotton root rot-infected cotton field near Edroy, TX in 2011. SRI = NIR / Red, NDVI = (NIR – Red) / (NIR + Red), MD = minimum distance, MAHD = Mahalanobis distance, ML = maximum likelihood, and SAM = spectral angle mapper.

Table 1 gives the estimates of infected and noninfected areas in pixels, hectares and percentage based on the six methods. Infected area estimates ranged from 40.5% with the maximum likelihood classifier to 45.8% with SRI. Table 2

presents the agreement values for the estimated infected areas between any two methods based on a pixel-to-pixel comparison. For example, the SRI method detected 222,261 pixels of infected areas and the minimum distance method identified 214,958 pixels of infected areas. The total number of common pixels identified by both methods was 214,486. Thus the agreement between the two methods was 214,486/222,261 = 0.965 with respect to the SRI method and 214,486/214958 = 0.998 with respect to the minimum distance method. The agreement values between any two methods ranged from 0.883 to 1.000, indicating a high degree of agreement among the six methods.

Table 1. Estimates of infected versus noninfected areas in pixels, hectares and percentage based on six methods from a four-band multispectral image of a 48.5-ha cotton root rot-infested cotton field near Edroy, TX in 2011.

Method[a]	Infected			Noninfected		
	Pixels	ha	(%)	Pixels	ha	(%)
SRI	222261	22.2	45.8	262631	26.3	54.2
NDVI	204239	20.4	42.1	280653	28.1	57.9
MD	214958	21.5	44.3	269934	27.0	55.7
MAHD	204087	20.4	42.1	280805	28.1	57.9
ML	196480	19.6	40.5	288412	28.8	59.5
SAM	217250	21.7	44.8	267642	26.8	55.2

[a] SRI = NIR / Red, NDVI = (NIR – Red) / (NIR + Red), MD = minimum distance, MAHD = Mahalanobis distance, ML = maximum likelihood, and SAM = spectral angle mapper.

Table 2. Agreement between each pair of the methods for identifying infected areas from a four-band multispectral image of a 48.5-ha cotton root rot-infested cotton field near Edroy, TX in 2011.

Method[a]	SRI	NDVI	MD	MAHD	ML	SAM
SRI	1.000	0.919	0.965	0.909	0.883	0.977
NDVI	1.000	1.000	1.000	0.960	0.948	1.000
MD	0.998	0.950	1.000	0.936	0.910	0.994
MAHD	0.989	0.961	0.986	1.000	0.957	0.981
ML	0.999	0.985	0.996	0.995	1.000	0.996
SAM	0.999	0.940	0.984	0.922	0.900	1.000

[a] SRI = NIR / Red, NDVI = (NIR – Red) / (NIR + Red), MD = minimum distance, MAHD = Mahalanobis distance, ML = maximum likelihood, and SAM = spectral angle mapper.

Table 3 summarizes the accuracy assessment results for the six classification maps. Overall accuracy ranged from 94.5% for the two vegetation indices to 96.5% for the minimum distance classifier, indicating that 94.5% to

96.5% of the image pixels were correctly identified in the classification maps. These results indicate that all six methods were accurate for indentifying root rot, though the minimum distance classifier provided the best result. Producer's and user's accuracy values ranged from 90.3% to 98.3% for the infected and noninfected classes. Producer's accuracy, a measure of omission error, indicates the probability of actual areas being correctly classified, while user's accuracy, a measure of commission error, indicates the probability that a category classified on the map actually represents that category on the ground. Based on the minimum distance method, the producer's accuracy for the infected class was 97.7%, while the user's accuracy for this class was 94.4%. In other words, 97.7% of the root rot areas on the ground were correctly identified as root rot on the classification map, but only 94.4% of the areas called root rot on the classification map were actually root rot on the ground.

Table 3. Accuracy assessment results for six classification maps generated from a four-band multispectral image of a 48.5-ha cotton root rot-infested cotton field near Edroy, TX in 2011.

Method[a]	Overall accuracy (%)	Overall kappa	Infected		Noninfected	
			PA	UA	PA	UA
SRI	94.5	0.889	97.7	90.3	92.1	98.1
NDVI	94.5	0.887	91.9	95.2	96.5	94.0
MD	96.5	0.929	97.7	94.4	95.6	98.2
MAHD	96.0	0.919	96.5	94.3	95.6	97.3
ML	95.5	0.908	91.9	97.5	98.3	94.1
SAM	96.0	0.919	97.7	93.3	94.7	98.2

[a] SRI = NIR / Red, NDVI = (NIR – Red) / (NIR + Red), MD = minimum distance, MAHD = Mahalanobis distance, ML = maximum likelihood, and SAM = spectral angle mapper.

CONCLUSIONS

Results from this study demonstrate that vegetation indices and supervised classifiers are effective tools for detecting cotton root rot from airborne multispectral imagery. Of the two vegetation indices and four classifiers examined in this study, the four classifiers appeared to be slightly better than the two vegetation indices. Although all four classifiers performed well, the minimum distance method provided the best result. More research is needed to evaluate the consistency and reliability of these methods and other spectral techniques for identifying root rot infection under diverse field and environmental conditions.

ACKNOWLEDGMENTS

This project was partly funded by Texas State Support Committee and Cotton Incorporated, Cary, NC. The authors wish to thank Adam Garcia of

Edinburg, TX and Fred Gomez of USDA-ARS at Weslaco, TX for taking the airborne imagery for this study and Jim Forward of USDA-ARS at Weslaco, TX for assistance in georeferencing the imagery.

REFERENCES

Campbell, J. B. 2002. Introduction to Remote Sensing, 3rd ed. The Guilford Press, New York.

Congalton, R. G. and K. Green. 1999. Assessing the Accuracy of Remotely Sensed Data: Principles and Practices. Lewis Publishers, Boca Raton, FL.

ERDAS. 2010. ERDAS Field Guide. ERDAS, Inc., Norcross, GA.

Ezekiel, W. N. and J. J. Taubenhaus. 1934. Cotton crop losses from phymatotrichum root rot. J. Agric. Res. 49(9):843-858.

Goldberg, N. P. 1999. Phymatotrichum root rot. Guide A-229. College of Agric. and Home Economics, New Mexico State Univ., Las Cruces, NM.

Isakeit, T., R. R. Minzenmayer, A. Abrameit, G. Moore, and J. D. Scasta. 2010. Control of phymatotrichopsis root rot of cotton with flutriafol. In Proc. Beltwide Cotton Conf., 200-203. National Cotton Council of America, Memphis, TN.

Isakeit, T., R. R. Minzenmayer, and C. G. Sansone. 2009. Flutriafol control of cotton root rot caused by *Phymatotrichopsis omnivora*. In Proc. Beltwide Cotton Conf., 130-133. National Cotton Council of America, Memphis, TN.

Jordan, C. F. 1969. Derivation of leaf area index from quality of light on the forest floor. Ecology 50(4):663-666.

Kruse, F. A., A. B. Lefkoff, J. W. Boardman, K. B. Heidebrecht, A. T. Shapiro, J. P. Barloon, and A. F. H. Goetz. 1993. The spectral image processing system (SIPS): Interactive visualization and analysis of imaging spectrometer data. Remote Sensing Environ. 44:145-163.

Nixon, P. R., D. E. Escobar, and R. L. Bowen. 1987. A multispectral false-color video imaging system for remote sensing applications. In Proc. 11th Biennial Workshop on Color Aerial Photography and Videography in the Plant Sciences and Related Fields, 295-305, 340. American Society for Photogrammetry and Remote Sensing, Bethesda, MD.

Richards, J. A. 1999. Remote Sensing Digital Image Analysis. Springer-Verlag, Berlin, 240 p.

Rouse, J. W., R. H. Haas, J. A. Shell, and D. W. Deering. 1973. Monitoring vegetation systems in the Great Plains with ERTS. In Proc. 3rd ERTS Symposium, 1: 309-317. NASA SP-351. Washington, D.C.: U.S. Government Printing Office.

Smith, H. E., F. C. Elliot, and L. S. Bird. 1962. Root rot losses of cotton can be reduced. Pub. No. MP361. Texas A&M Agricultural Extension Service, College Station, TX.

Walla, W. J., and E. Janne. 1982. Controlling cotton root rot on ornamental plants. Publ. No. TAEX L-2056. The Texas A&M Univ. System, Texas Agric. Ext. Serv., College Station, TX.

Yang, C. 2010. A high resolution airborne four-camera imaging system for agricultural applications. ASABE Paper No. 1008856, American Society of Agricultural and Biological Engineers, St. Joseph, MI.

Yang, C., C. J. Fernandez, and J. H. Everitt. 2005. Mapping Phymatotrichum root rot of cotton using airborne three-band digital imagery. Transactions of the ASAE 48(4):1619-1626.

Yang, C., C. J. Fernandez, and J. H. Everitt. 2010. Comparison of airborne multispectral and hyperspectral imagery for mapping cotton root rot. Biosystems Engineering 107:131-139.

Yang, C., G. N. Odvody, C. J. Fernandez, J. A. Landivar, R. R. Minzenmayer, and R. L. Nichols. 2011. Using multispectral imagery to monitor cotton root rot expansion within a growing season. In Proc. Beltwide Cotton Conf., 559-568. National Cotton Council of America, Memphis, TN.